ISBN: 978-3-95450-249-3 ISSN: 2673-5350 doi: 10.18429/JACoW-IBIC2024-TUP25

DEVELOPMENT OF STRIPLINE-TYPE BEAM POSITION MONITOR SYSTEM FOR CSNS-II*

M. A. Rehman†, R. Yang‡, Z. Xu, R. Liu, L. Fang, B. Zhang, W. Huang, S. Wang
Institute of High Energy Physics, Chinese Academy of Sciences (CAS), Beijing, China
also at China Neutron Spallation Source, Dongguan, China

Abstract

As part of the CSNS-II upgrade, the H^- LINAC beam energy will be increased from 80 MeV to 300 MeV using superconducting cavities. To accurately measure beam position, phase, and energy, the stripline-type Beam Position Monitors (BPM) are essential. The shorted-type stripline BPM was chosen for this upgrade due to its excellent S/N ratio and rigid structure. As space is limited in the LINAC's superconducting section, the BPMs must be embedded in the quadrupole magnet. Two prototypes, with inner diameters of 50 mm and 96 mm, were designed using numerical simulation codes and manufactured for beam testing. This paper will detail the simulation, design, and beam test results of the prototype BPM for CSNS-II.

INTRODUCTION

The China Spallation Neutron Source (CSNS) [1, 2] provides intense pulsed neutron beams for a wide range of scientific research and industrial applications. The CSNS accelerator complex comprises an 80 MeV Linac, a 1.6 GeV Rapid Cyclic Synchrotron (RCS), and a solid tungsten target station. The 80 MeV H^- beam from the Linac is injected into the RCS using a multi-turn charge exchange process. The RCS then increases the beam energy to 1.6 GeV, with a beam intensity of 1.56×10^{13}, delivering a beam power of 100 kW. The beam power has been raised to 160 kW with the incorporation of harmonic cavities [3].

The power of the beam will be increased to 500 kW for CSNS-II. As part of the CSNS-II upgrade, the beam energy in the Linac will be raised from 80 MeV to 300 MeV using superconducting cavities. To ensure precise measurement of beam position, phase, and energy in the new superconducting section of the Linac, a new stripline-type Beam Position Monitoring (BPM) system is crucial. The shorted-type stripline BPM has been selected for this upgrade because of its excellent signal-to-noise ratio and rigid structure. Due to limited space in the Linac's superconducting section, the BPMs must be embedded in the quadrupole magnets. Two prototypes, with inner diameters of 50 mm and 96 mm, were designed using numerical simulation codes and manufactured, one BPM of 96 mm diameter was also tested with the beam. The parameters of CSNS and CSNS-II are described in Table 1.

Table 1: CSNS and CSNS–II RCS Parameters

Parameters	CSNS	CSNS–II	Units
Beam Power	100	500	kW
Injection Energy	80	300	MeV
Bunch Frequency	324	324/648	MHz
Bunch length	20	8	ps
Ring Circumference	227.92	227.92	m
Extraction Energy	1.6	1.6	GeV
Repetition Rate	25	25	Hz
Number of Bunches	2	2	
RCS Beam Intensity	1.56×10^{13}	7.8×10^{13}	ppb

BEAM POSITION MONITOR

Two stripline BPMs will be placed into the quadrupole magnets after the normal conducting Drift Tube Linac (DTL). In the spoke cavity region, where beam energy will be increased from 80 MeV to 165 MeV, 10 BPMs will be placed in every other quadrupole magnet of the FODO lattice. The elliptical cavity region will boost the beam energy up to 300 MeV and contain 8 BPMs embedded in the quadrupole magnets. In the drift section (LRBT), after the elliptical cavity region, 10 BPM will be placed, and one BPM of small diameter will be placed at the injection point. Table 2 represents the BPM design parameters.

Table 2: Superconducting Section BPM Parameters

Parameters	Values
Position Accuracy	1% of R
Position Resolution	50 μm
Phase Accuracy	1°
Phase resolution	0.2°
Meas. Range	R/2

The shorted stripline-type BPM has been chosen for CSNS-II owing to its rigid structure and high S/N ratio. Due to the stringent space restriction in LINAC's superconducting section, BPMs must be embedded inside the quadrupole magnet. Therefore, the transverse and longitudinal size and shape of the BPMs are strictly restricted. In shorted-stripline BPM, four stripline electrodes with $\pi/2$ rotational symmetry are installed in the vacuum pipe, with their ends grounded to the vacuum duct.

The passage of a charged particle induced image current on a stripline is proportional to the distance between the electrode and the beam, beam intensity, the electrode's opening angle, and the stripline's length. If the character-

* Work supported by National Science Foundation for Young Scientists of China (12305166).
† rehman@ihep.ac.cn
‡ yangrenjun@ihep.ac.cn

ISBN: 978-3-95450-249-3 ISSN: 2673-5350 doi: 10.18429/JACoW-IBIC2024-TUP25

istic impedance feedthrough is equal to the characteristic impedance of the stripline ($Z_0 = 50\,\Omega$), the voltage at the readout feedthrough port of a stripline electrode of length l is given as follows [4]:

$$V(t) = \frac{Z_{strip}}{2}\frac{\alpha}{2\pi}\left(\frac{e^{-t^2}}{2\sigma^2} - \frac{e^{\left(t-l\left(\frac{1}{c}+\frac{1}{v}\right)\right)^2}}{2\sigma^2}\right) I_0, \qquad (1)$$

where α is the opening angle of the stripline electrode, I_0 the beam current and v is the velocity of the beam. The optimized electrode length at a given beam velocity can be calculated as $l = \left(\frac{\pi c v}{\omega(c+v)}\right)$. Figure 1 (a) shows the perspective view of the BPM embedded inside the quadrupole magnet, and Fig. 1 (b) illustrates the transverse cross-sectional view of the stripline BPM.

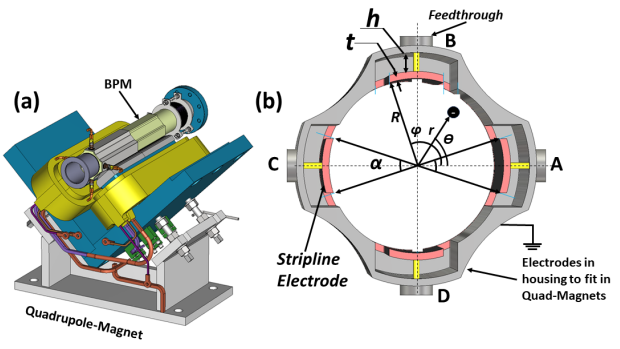

Figure 1: (a) A perspective view of the BPM embedded inside quadrupole magnet. (b) The transverse cross-sectional view of the stripline BPM.

The velocity of the beam continuously changes as the beam gets accelerated through the spoke cavity and elliptical cavities. Therefore, each BPM should have an optimized length of stripline electrodes according to incoming beam velocity. To simplify the mechanical construction and reduce cost, a constant length of stripline electrodes has been chosen in the spoke cavity and elliptical cavity region. The value of the β in spoke and elliptical cavities are 0.46 and 0.65, respectively. We have chosen the length of stripline electrodes, which results in 143.6 mm and 183.2 mm for spoke and elliptical cavities regions, respectively. For the LRBT region, the length of the electrodes is also 183.2 mm, since there is no constraint on length for the BPM located at the injection point, the length was chosen 231.5 mm. Figure 2 shows the optimized length of electrodes at different beam velocities and bunching frequencies.

In the case of the low β beams, the beam bunches have longitudinal components, and the Transverse Electro-Magnetic (TEM) mode assumption cannot be applied. The full 3-D Laplace equation has to be solved. The position sensitivity of pairs of electrodes in the case of low beta beams also depends on beam energy and RF frequency. The sensitivity in logarithmic ratio form can be calculated as following [5]:

$$\left(\frac{V_r}{V_l}\right)_{dB} = \frac{160}{Ln(10)}(1+G)\frac{\sin(\alpha/2)}{\alpha}\frac{x}{R}, \qquad (2)$$

where V_r and V_r are measured voltages from the right and the left stripline, respectively. And G is the correction factor and can approximated as [5]:

$$G = 0.139\left(\frac{\omega R}{\beta\gamma c}\right)^2 - 0.0145\left(\frac{\omega R}{\beta\gamma c}\right)^3, \qquad (3)$$

where α is the electrode opening angle, R is the radius of the beam duct, x is the beam position and ω is the angular frequency. Whereas in Eq (3), c is the velocity the light, β and γ are the Lorentz factor. The beam β ranges from 0.38 to 0.65 in superconducting section section. The above equations are valid in first-order approximation, assuming that the transverse offset is much smaller than the vacuum duct radius. The beam transverse position from the BPM is given by $x = k\,(V_r/V_l)_{dB}$, where k is a calibration constant, or more accurately, could be found from the wire mapping.

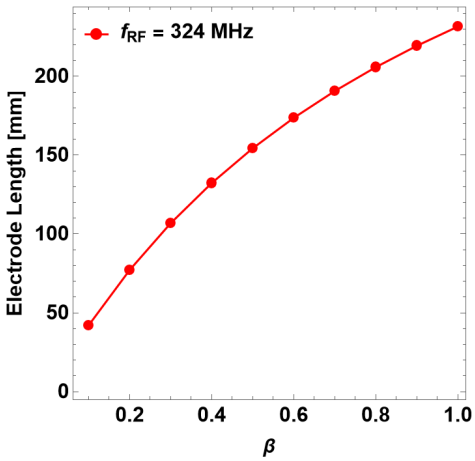

Figure 2: The Lorentz factor versus BPM electrode length in the different sections of CSNS–II LINAC.

NUMERICAL SIMULATION

The impedance of cables, feedthrough, and stripline electrodes must be matched to avoid signal reflection and deformation at the upstream readout feedthrough. The feedthrough is weldable and commercially available with an SMA-type connector of 50 Ω impedance. Therefore, the stripline electrode must be optimized for the 50 Ω impedance. The available space between the poles of the quadrupole magnet fixed the width of the stripline. The inner diameter of the vacuum duct along the superconducting section is 50 mm, 96 mm and 52 mm. The stripline electrodes are placed outside the beam pipe aperture to preserve the accelerator acceptance.

The thickness was set at 2 mm to ensure the stripline electrode's mechanical strength. The gap between the stripline electrode and vacuum duct was optimized to obtain the 50 Ω impedance. The characteristic impedance of the

ISBN: 978-3-95450-249-3 ISSN: 2673-5350 doi: 10.18429/JACoW-IBIC2024-TUP25

stripline electrode was calculated using a numerical code CST-MW [6]. Figure 3 shows the feedthrough and stripline electrode impedance calculations, where g_h is the gap between the electrode and vacuum duct, which has been varied to obtain the 50 Ω impedance.

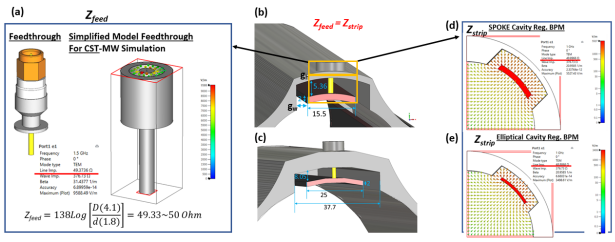

Figure 3: Characteristics impedance of feedthrough and stripline of BPM.

Figure 4 shows the typical output signal of a stripline electrode and its Fourier transform; black lines show the scenario of impedance mismatch between feedthrough and stripline electrodes, which results in an unbalanced bipolar signal and also shows a large reflection. Whereas green lines in Fig. 4 depicts the case of impedance matching, which shows the balanced bipolar signal.

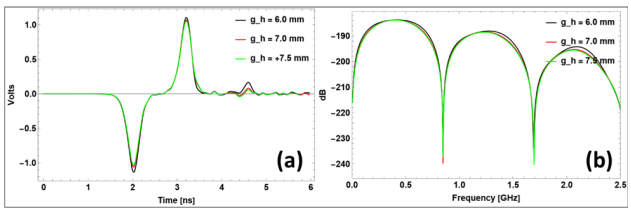

Figure 4: The typical bipolar signal of the stripline BPM in time and frequency domain.

MECHANICAL DESIGN

Table 3 describes the optimized geometrical parameters of BPMs. In Table 3, T1 and T2 refer to the BPM in the spoke and elliptical cavities region, respectively. T3 and T4 refer to the BPM in LRBT and injection location BPMs, respectively.

Table 3: Geometrical Parameters of BPMs

Parameters	T1	T2	T3	T4
Opening Angle	36.12	25.3	40.0	54.0
Stripline Length	143.6	183.2	183.2	231.5
Stripline Thickness	2.0	2.0	2.0	2.0
Inner Diameter	50.0	96.0	96.0	52.0
Quad Embed	Yes	Yes	No	No

Two prototype BPMs for the spoke and elliptical cavities region were manufactured. The BPM are manufactured using SUS316L, which exhibits a low magnetic permeability of approximately 1.05. The outer body of the BPM is designed to accommodate the monitor inside the quadrupole magnet.

POSITION CHARACTERISTICS

The position characteristics of proto-type BPMs were evaluated using the wire calibration system. The third-order polynomial fit was used to correct the beam position nonlinearities as follows:

$$x_{BPM} = \sum_{i,j=0}^{3} (c_{i,j} x_{raw}^{i} y_{raw}^{j}), \quad (4)$$

$$y_{BPM} = \sum_{i,j=0}^{3} (c_{i,j} y_{raw}^{i} x_{raw}^{j}), \quad (5)$$

where x_{BPM} and y_{BPM} are the corrected transverse position, $c_{i,j}$ is the coefficient of the polynomial and x_i^{raw} and y_j^{raw} are calculated using the following formula: $x_{raw} = \frac{V_R - V_L}{V_R + V_L}$ and $y_{raw} = \frac{V_U - V_D}{V_U + V_D}$. V_R, V_L, V_U and V_D are voltage from the right, left, up and down electrodes of the BPMs, respectively. The mapping results and absolute errors are shown in Figs. 5 (a) and (b), respectively.

The spoke cavity region BPMs maximum absolute error reduces to a few, about 40 µm with the correction of a polynomial of third-order as shown in Fig. 5 (b). In the case of elliptical cavity region BPM error, the error to the 48 µm as mentioned. The analysis shows that the maximum error is about 50 µm, which is less than the 1% of half of the radius, meeting the requirements.

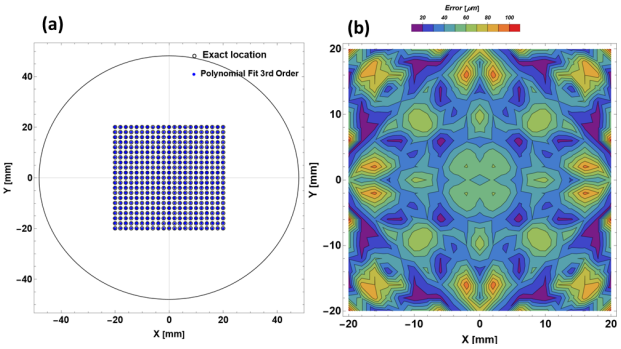

Figure 5: Two-dimensional polynomial correction and remaining error to the simulated positions in CST-PS for spoke cavity region BPM.

BEAM EXPERIMENT

For the CSNS LRBT region, the inner diameter of the beam duct is 70 mm. Therefore, only the BPM of an inner diameter of 96 mm could be tested with the beam. Due to abrupt changes in beam duct diameter, wakefield could arise and appear as signal deformation. The tapered structure was added in BPM's upstream and downstream directions

ISBN: 978-3-95450-249-3 ISSN: 2673-5350 doi: 10.18429/JACoW-IBIC2024-TUP25

to avoid signal deformation. Figure 6 shows the signal deformation with an abrupt change in the beam pipe diameter and mitigation of this effect with the tapper structure.

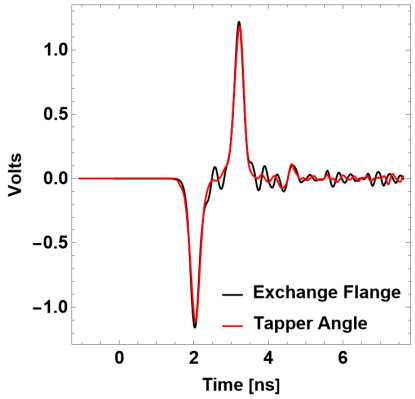

Figure 6: The signal deformation occurs due to abrupt change of beam aperture. The tapper structure has been used to mitigate this issue.

Figure 7 shows the installed BPM model and photograph of the installed BPM on the beamline.

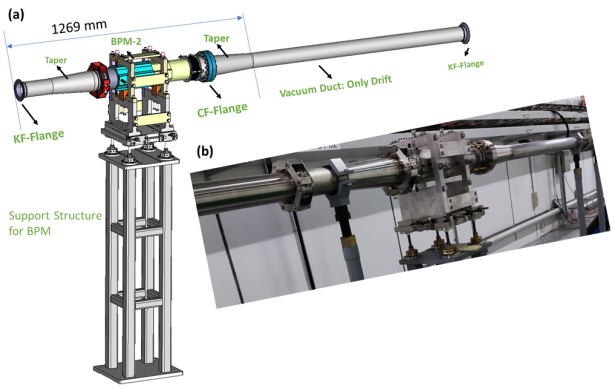

Figure 7: (a) The model of the installed BPM with taper structure in upstream and downstream directions.(b) The photo of the BPM at the beamline.

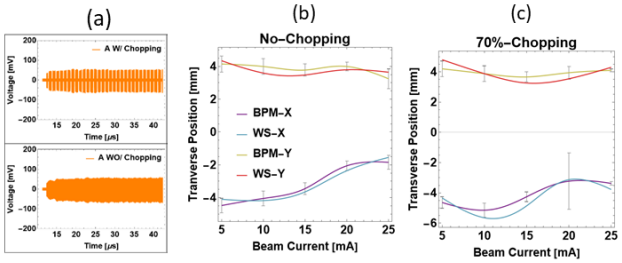

Figure 8: (a) The BPM signal from the with 70% beam chopping rate and without chopping. (b) The The transverse position of the beam as function of the beam current without chopping. (c) The transverse position of the beam as function of the beam current with chopping.

The BPM system has been tested with the beam. During the beam test, the energy of the beam was 80 MeV, the beam energy remains constant in the LRBT section. The beam peak current was 5 mA with a macro pulse width of 50 µs. An example signal from BPM four electrode is shown in Fig. 8. In Fig. 8 (a) and (b), the top graph shows the measured continuous 324 MHz beam signal with a 70% chopping rate from BPM, whereas bottom graph shows the without chopping. Figures 8 (b) and (c) illustrate the horizontal and vertical beam position from the newly installed BPM as a function of the beam current without and with 70% beam chopping.

SUMMARY

As a part of the CSNS-II power upgrade, the H^- injector Linac beam energy will be increased to 300 MeV by using superconducting cavities. The stripline-type BPM system has been simulated, design and prototype was manufactured. The length of the BPMs electrodes were optimized according to the beam energy. Through numerical simulations the geometry of the BPM has been optimized to obtain 50 Ω impedance of the electrodes. Two prototype BPMs were manufactured, the wire mapping of the BPMs were performed in order to characterize the position reading capabilities. Position accuracy of better than 50 µm has been achieved in the wire test. One BPM with adequate inner diameter to the existing beam line was tested with beam, and the beam transverse position along the injector LIANC was measured.

ACKNOWLEDGMENTS

We thank Dr. Jun Peng for the fruitful discussion.

REFERENCES

[1] J. Wei *et al.*, "China Spallation Neutron Source: Design, R & D and Outlook", *Nucl. Instrum. Methods Phys. Res., Sect. A*, vol. 600, no. 1, pp. 10-13, Feb. 2009. doi:10.1016/j.nima.2008.11.017

[2] S. Wang *et al.*, "Introduction to the Overall Physics Design of CSNS Accelerators", *Chinese Physics C*, vol. 33, no. S2, pp. 1-3, Jun. 2009. doi:10.1088/1674-1137/33/S2/001

[3] L. Huang *et al.*, "Intense Beam Issues in CSNS Accelerator Beam Commissioning", in *Proc. HB'23*, Geneva, Switzerland, Oct. 2023, pp. 16–22. doi:10.18429/JACoW-HB2023-MOA1I3

[4] P. Forck, P. Kowina, and D. Liakin. "Beam Position Monitors", in *CAS- CERN Accel. School: Beam Diagnostics*, CERN, Geneva, Switzerland, 2009. doi:10.5170/CERN-2009-005.187

[5] R. E. Shafer, "Beam Position Monitor Sensitivity for Low-β Beams", *AIP Conf. Proc.*, vol. 319, pp. 303-308, 1994. doi:10.1063/1.46975

[6] CST-Studio, https://www.3ds.com/products/simulia/cst-studio-suite